

XMM-Newton CCF Release Note

XMM-CCF-REL-156

Improved Vignetting Correction by refining the XMM optical axis.

M. Kirsch

January 27, 2004

1 CCF components

Name of CCF	VALDATE	List of Blocks changed	CAL VERSION	XSCS flag
XMM_MISCDATA_0020	1999-01-01T00:00:00	PARAM_ID	3.152	NO
XMM_BORESIGHT_0017	2000-01-01T00:00:00	EULER_PHI, EULER_THETA, EULER_PSI	3.152	NO

2 Changes

We discovered that the optical axis for the three EPIC instruments do not agree with the values in the CCF. The real optical axis was determined with various methods (see D. Lumb et al. TBP). The results of the different methods agreed within the errors. Finally the values of the method with the smallest errors have been used for a new XMM_MISCDATA_0020 CCF. The new optical axis position required also a new XMM_BORESIGHT CCF which holds for each instrument a triple of three angles describing the misalignment of the respective instrument boresight with respect to the satellite coordinate frame. Using the OMC2/3 field new BS misalignment angles for all the three cameras have been calculated. We verified the improvement of the vignetting correction with observations of the SNR 3C58 and the Coma cluster.

2.1 XMM_MISCDATA: PARAM_ID

The values OPTIX_X and OPTIX_Y for all cameras have been changed. Table 1 shows the old and new values. Table 2 show the shift with respect to the old position of the optical axis.

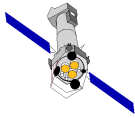


Table 1: Old and new position of optical axis

Camera	OPTIX_X (old)	OPTIX_X (new)	OPTIX_Y (old)	OPTIX_Y (new)
MOS1	300	305	300	291
MOS2	300	325	300	243
pn	39	23	188	183

numbers are given in RAW coordinates (PIXCORD)

Table 2: Shift of optical axis

Camera	shift_X	shift_Y
MOS1	-5.5	9.9
MOS2	-27.5	62.7
pn	65.6	20.5

numbers are given in arcsec

2.2 XMM_BORESIGHT: EULER_PHI, EULER_THETA, EULER_PSI

The new optical axis position required also a new XMM_BORESIGHT CCF which holds for each instrument a triple of three angles describing the misalignment of the respective instrument boresight with respect to the satellite coordinate frame.

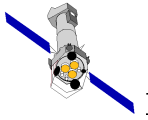
Table 3: New and old BS misalignment angles

Camera	PHI(old)	PHI(new)	THETA(old)	THETA(new)
MOS1	3.141933497	3.14195955728	-0.0003341476707	-0.00028640244
MOS2	3.141990024	3.14168078953	-0.0002931450122	-0.00016189813
pn	3.1419488369	3.14185930817	-0.000256345242160023	-0.00056853041

Camera	PSI(old)	PSI(new)
MOS1	0.00156197284	6.1831991E-06
MOS2	-0.0030311789	-0.0050972434
pn	0.00469273	0.0037681627

numbers are given in rad

Using the OMC2/3 field new BS misalignment angles for all the three cameras have been calculated with *epicbscalgen*. Table 3 shows the old and new values for the misalignment angles.



3 Scientific Impact of this Update

The changes do not effect the XMM-astrometry. We checked that with the OMC2/3 field data. Crosscorrelation with the 2MASS catalog show that the astrometry is still within 1 arcsec (r.m.s.) for all three cameras. See Figure 1. Further investigations by SSC are underway.

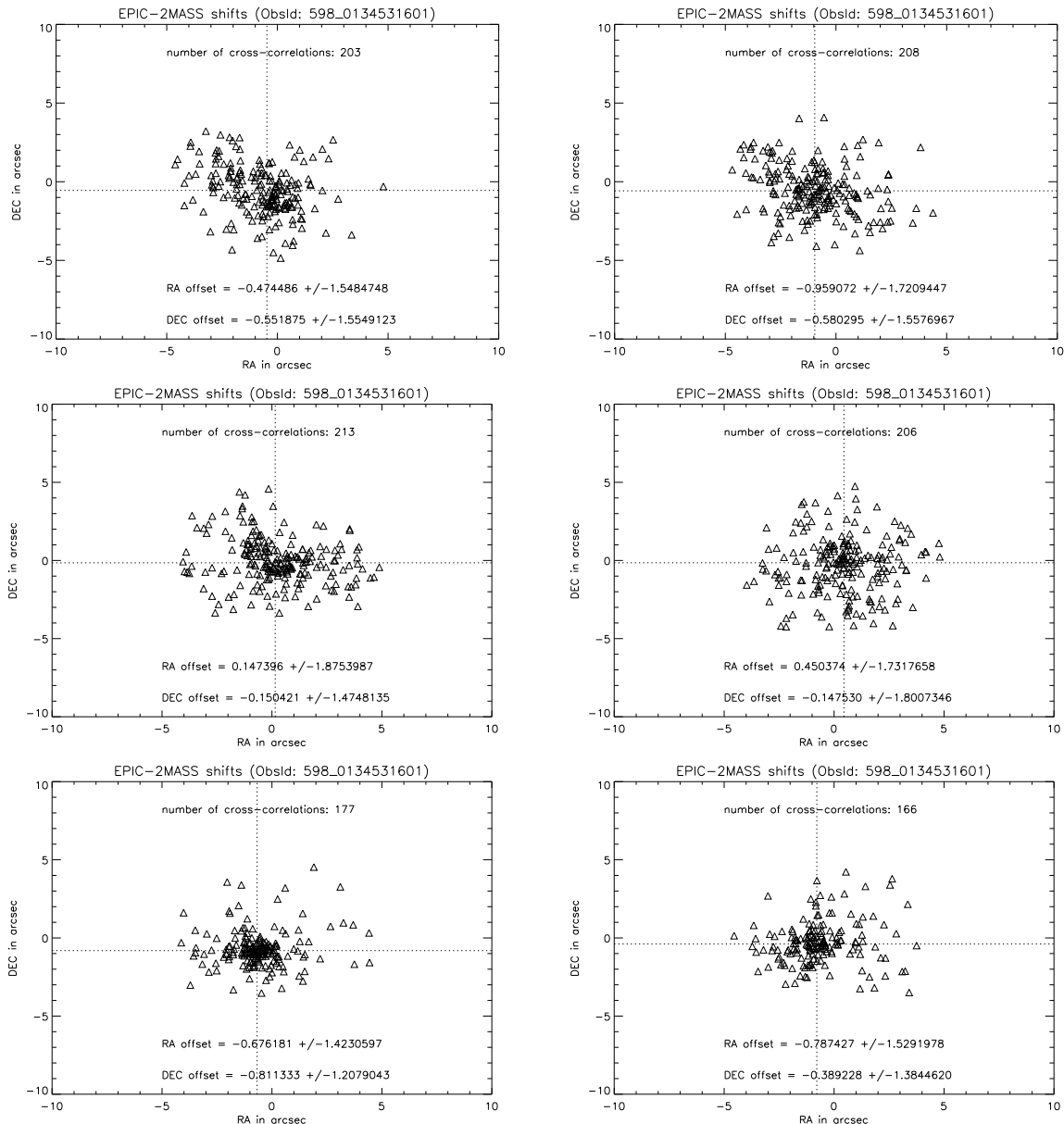
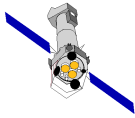


Figure 1: 2MASS EPIC crosscorrelation with old (left) and new (right) CCFs for MOS1 (top), MOS2 (centre), pn (bottom)

Note: The new XMM_MISCDATA_0020 and XMM_BORESIGHT_0017 do only work in combination with the new SAS 6.0. Errors in attcalc have been spotted and corrected. The old attcalc would only access part of the new CCFs in the correct way causing wrong coordinates for the sources.



4 Estimated Scientific Quality

The new consideration of the right optical axis position improves the vignetting correction. However the vignetting correction itself has not changed at all, the only difference is, that it is now applied for correct off axis angles, that could not be calculated correctly before due to the wrong information for the optical axis. This improves differences in flux for off axis sources for each camera from $\pm 14\%$ to $\pm 5\%$.

5 Test procedures & results

5.1 OMC2/3

The CCFs have been tested on the OMC2/3 fields of the revolutions 237 and 598 for the astrometry check (see Fig.1).

5.2 Coma Cluster

The Coma cluster of galaxies is one of the brightest diffuse X-ray objects on the sky, filling the field of view of XMM-Newton detectors. This cluster was observed with different positional angle. For check of the vignetting correction the same regions on the sky, which due to the differences in the positional angle of ~ 120 degrees end up at different positions relative to the optical axis, were analysed for both observations.

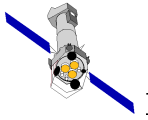
The original calibration introduced a 14% r.m.s. scatter in the surface brightness data, while the revised calibration decreases the r.m.s. to 3-5%, comparable with the statistical noise. This result is consistent with the large r.m.s. scatter found in pn-MOS1 comparison of serendipitous sources in XMM-SOC-CAL-TN-0023.

The one-dimensional scatter of the flux-ratio for the different regions can be used as an indication for the quality of the vignetting correction. The mean value and the dispersion in r.m.s. give the accuracy of the vignetting for all three cameras (see Table 4).

Table 4: Residual dispersion in the vignetting calibration.

camera	mean	Dispersion, %
MOS1	1.003054	5.60
MOS2	1.006452	5.00
pn	1.006208	3.58

Note that the mean value of 1.000 is not enforced.



5.3 SNR 3C58

For the improvement in the vignetting area we tested on the 3C58 observations of revolution 505 and 506, that have been placed at different off axis angles and azimuths. The 3C58 data show an improvement from $\pm 10\%$ to $\pm 3-4\%$ for the accuracy of flux for the same source off axis or at the optical axis position.

Figure 2 shows the improvement for the 3C58 observations.

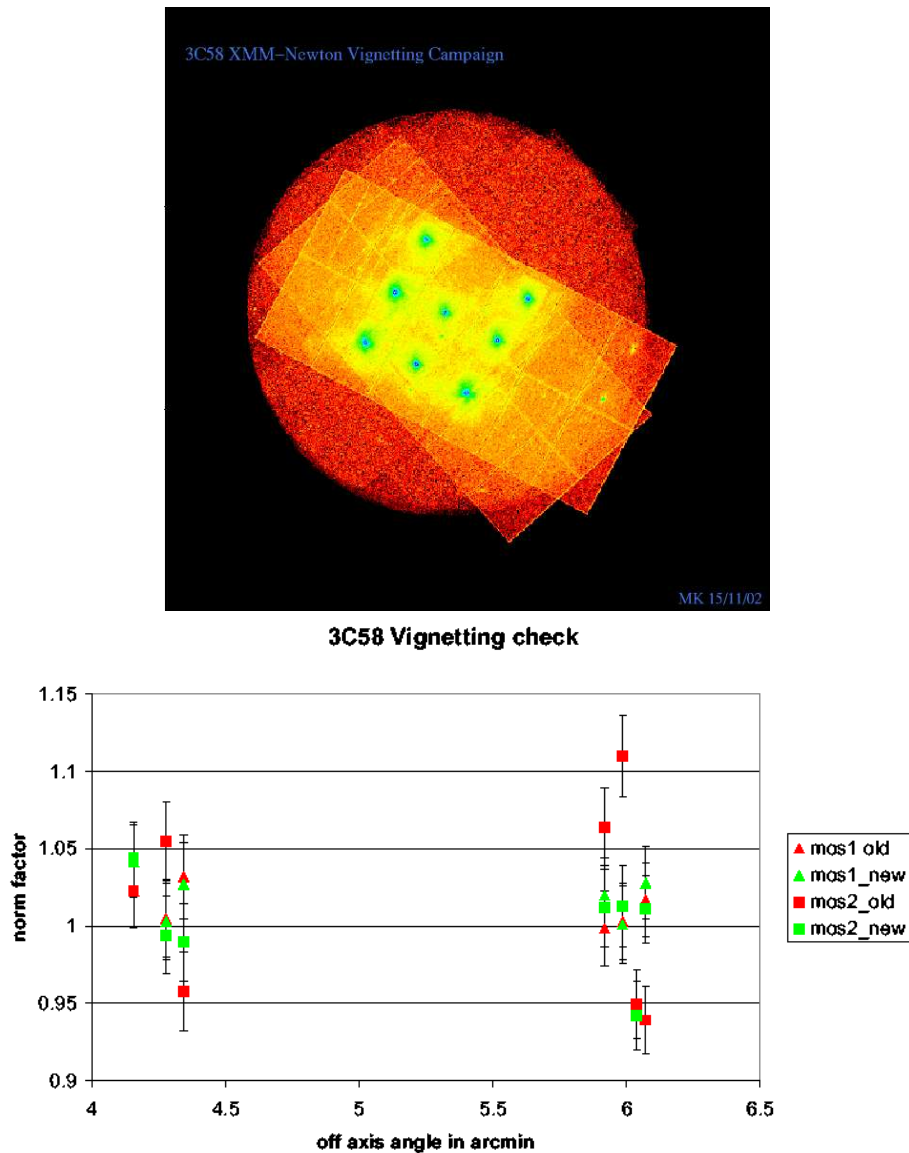
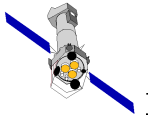


Figure 2: Differences in flux for 3C58 off axis measurements. The data has been fitted with the model $\text{const} * (\text{wabs} * \text{powerlaw})$. The constant was fixed to 1 for the central measurement. The data point with the factor of 0.94 at 6 arcmin shows no improvement, since the source was falling onto a CCD gap, where recovering of flux is not trivial anymore.



6 Expected Updates